LBL--25694

DE89 006659

LOW CAPACITANCE LARGE VOLUME SHAPED-FIELD GERMANIUM DETECTOR*

P. N. Luke, F. S. Goulding, N. W. Madden and R. H. Pehl

Engineering Division
Lawrence Berkeley Laboratory
One Cyclotron Rd.
Berkeley, California 94720 U.S.A.

*This work was supported by the Director's Office of Energy Research, Office of Health and Environmental Research, U.S. Department of Energy under Contract No. DE-AC03-76SF00098.

LOW CAPACITANCE LARGE VOLUME SHAPED-FIELD GERMANIUM DETECTOR

P. N. Luke, F. S. Goulding, N. W. Madden and R. H. Pehl

Engineering Division
Lawrence Berkeley Laboratory
One Cyclotron Rd.
Berkeley, California 94720 U.S.A.

Abstract

A large volume (150 cm^3) germanium detector with a full-depletion capacitance of only ≈ 1 pf has been fabricated. The effect of impurity space-charge was utilized to obtain an appropriate electric field distribution in the detector so that carriers are collected on a small area electrode. Detectors based on this principle are capable of very low noise operation and have immediate applications in direct detection dark matter particle experiments. Detector pulse shapes and carrier trapping effects were also examined for possible applications involving higher energy radiations.

Introduction

Large volume high-purity germanium detectors, usually in the form of closed-end coaxes, are routinely used in high-resolution gamma ray spectroscopy applications. Figure 1 shows the structure of a typical reverse electrode coaxial detector. It is in the shape of a cylinder with a hole bored from one end to form the n^+ electrode. The opposite (closed) end and the curved outer surface is covered with a p^+ electrode. Reverse electrode coaxial detectors are mostly fabricated from n-type materials. Conventional electrode coaxial detectors, which are usually made from p-type material, have the same geometry but with the opposite electrode configuration. The coaxial geometry allows large volume single detectors to be produced with minimum charge collection distances, reasonably low depletion voltages, and thin, uniform entrance windows. Typical coaxial detectors have outer diameters of about 5 - 6 cm and comparable lengths. The minimum diameter for the central electrode is limited in practice to about 6 mm. The capacitance of such detectors is in the range of 20 pf. Because of their relatively large capacitances, spectrometers utilizing large-volume coaxial germanium detectors have electronic noise greater than about 500 eV FWHM. For the spectroscopy of high energy photons (> 100 keV), for which large volume detectors are primarily used, such a noise level does not make a major contribution to the energy resolution which is dominated by statistics of charge production in the detector. However, for applications where low energy performance is important, the relatively high electronic noise is a serious limitation.

One such application that requires the lowest electronic noise and the largest detector mass is the search for weakly interacting massive particles using "direct" detection. The existence of these particles has been proposed to account for the dark ("missing") matter in the universe [1]. It may be possible to detect these particles through their elastic interactions with nuclei in a detector [2]. Since these particles have typical velocities of only ~ 300 km/sec, the kinetic energy transferred to the nuclei are small (up to a few keV). In addition, for the same kinetic energy, heavy nuclei produce far less ionization than electrons. Therefore, detectors with very low detection thresholds are required. The low probability of such interactions of these particles with detector material makes it essential to employ large detectors. Figure 2 shows the predicted interaction rate as a function of equivalent electron energy deposited in germanium for various particle masses. Useful limits on particle masses have already been obtained by us using standard

coaxial germanium detectors which were originally intended for double beta decay experiments [3]. These detectors have electronic noise of ≈ 1.2 keV FWHM, corresponding to an energy threshold of ≈ 3 keV. Data collected so far have produced an upper limit on the particle mass of ≈ 15 GeV/c^2. Significant improvements on the mass limit will be obtained if the detection threshold can be substantially lowered; to achieve this result it is necessary to reduce the detector capacitance. We report here the development of a very low capacitance, large volume germanium detector which, although is aimed primarily for the dark matter particle search, possesses unique properties that may be relevent for many other applications as well.

Shaped-Field Detector

Examining the structure of a coaxial detector, it is obvious that its capacitance can be decreased by decreasing the diameter of the inner electrode and by shortening it. In the limit when the central electrode is reduced to a a small area contact at the open end of the detector, as shown in Fig.3, the capacitance will be lowest. As long as the outside dimensions of the detector are much larger than the central electrode, the capacitance of a fully depleted detector will depend mainly on the size of the central electrode. If we consider the central electrode to be hemispherical in shape with radius r, the detector capacitance can be expressed as

$$C \approx 2\pi K \varepsilon_0 r$$

where $\varepsilon_0 = 8.85 \times 10^{-12}$ farad/m is the free space permittivity and K is the dielectric constant of the material. For a large volume germanium detector with r = 1 mm, the capacitance will be only ≈ 0.9 pf.

For a detector with such a geometry to function properly, an appropriate internal electric field must be established such that carriers produced by radiation interacting anywhere in the detector can be efficiently collected on the electrodes. This can be achieved by using the space-charge that exists in a depleted detector due to the presence of impurities in the material. Germanium detectors that utilize impurity space-charge effects to establish built-in electric fields have been developed earlier. These were intended mainly as low-energy detectors which have thicknesses of several mm. They were studied as position-sensitive detectors [4] and as large area low capacitance detectors [5]. The present work represents an extension of the same principle to large volume detectors.

Consider a detector with the structure shown in Fig.3. With the application of reverse bias, a depletion region will form, starting from the p^+-n junction. With increasing bias the undepleted region will shrink towards the axis of the detector and also away from the closed end. At full depletion, an electric field is established in the detector that would cause holes to drift to the p^+ electrode and electrons to drift radially towards the axis. However, if material having a uniform net impurity concentration is used, there is no significant axial field present except near the closed end; therefore, electrons will not drift well to the n^+ electrode. To increase the axial field, one could taper the detector such that it has a smaller diameter at the closed end. The disadvantage of this method is that substantial volume of the detector is lost. Alternatively, one can maintain the right cylinder geometry and use material with an axial impurity gradient. Such material is readily available as a result of the segregation of impurities during the crystal growth process [6]. In fact, many of the crystals used for n-type coaxial detectors have axial impurity gradients suitable for this application.

For our test detector, we have chosen a germanium crystal with diameter and length each measuring 58 mm. It has a net donor concentration that ranges from about 0.7×10^{10} cm^{-3} at one end to 1.5×10^{10} cm^{-3} at the other. The closed end of the detector was formed from the end

with the lower impurity concentration. The p^+ electrode was formed by boron ion implantation and the n^+ electrode by lithium diffusion. The small disk-shaped n^+ electrode has a diameter of 2 mm and is about 0.5 mm thick.

The electric field distribution in the detector can be calculated using the Poisson equation. For the present case, the equation cannot be solved in closed form but can be calculated numerically with a computer using the finite difference method. The result of such a calculation of the electric potential for electrons for the test detector is plotted in Fig.4. The impurity concentration gradient was assumed to be linear. A bias of 3200 V, which is slightly above the full depletion bias of the detector, was used in the calculation. As can be seen, electric field is formed inside the detector to cause the electrons to be collected on the small n^+ electrode. The electric field strengths are reasonably high throughout most of the detector volume. The weakest field ($\approx$ 200 V/cm) occurs near the n^+ electrode along the detector axis.

Figure 5 shows the measured capacitance of the test detector as a function of bias. As expected, the capacitance dropped to a very low value of $\approx$ 1 pf at full depletion. The additional decrease in capacitance beyond full depletion (> 3000 V) is most likely due to further depletion into the n^+ electrode which may have a diffusion 'tail' with low donor concentration.

The detector was scanned at various positions using a collimated ^{241}Am 59.5 keV gamma-ray source. Signals were observed in all cases, implying that carriers are collected throughout the whole volume of the detector. However, because of the long charge collection distances and the presence of regions with relatively low drift fields, charge trapping effects were greatly enhanced. Figure 6 shows ^{241}Am spectra taken at two scan positions; that taken with the source impinging near the closed end (with longer charge collection distance) shows a decrease of about 3% in the charge collected compared to that with the source impinging near the open end. Since the signals are due almost entirely to electron motions, the loss is due to electron traps. Although much less pronounced, similar electron trapping effects are commonly observed in reverse electrode coaxial detectors.

In the search of dark matter interactions, the expected low energy events should exhibit a continuous energy distribution. Therefore, good energy resolution is unimportant, and the trapping effects observed here are not significant. Instead, the key issue here is the electronic noise. In our initial tests using conventional resistive feed-back electronics with an in-can FET (2N4416), a noise level of 270 eV FWHM was obtained at an amplifier peaking time of 8 μs. The detector leakage current was $\approx$ 2 pA; lower current is possible with further processing. With detector capacitance of only $\approx$ 1 pf, an electronic noise level of $\lesssim$ 100 eV FWHM should be achievable using de-mounted FET and pulsed-reset electronics. Systems using such detectors would therefore provide a very significant factor of ~ 5 decrease in the energy threshold compared to that using coaxial detectors. This would reduce the mass limit on the relevant dark matter particle candidates to ~ 5 GeV/c^2.

Pulse Shapes

Although the low capacitance of the shaped-field detector is not important for the spectroscopy of high-energy photons, the shapes of the induced signals are such that shape discrimination can be used to differentiate between single point and multiple point interaction events.

The instantaneous current induced at an electrode of a detector due to the movement of a point charge q can be written as [7]:

$$i = q\,\vec{v}(\vec{E}) \cdot \vec{E}_0$$

where $\vec{v}(\vec{E})$ is the velocity of the point charge, and $\vec{E}_0$ is the hypothethical electric field that would exist inside the detector under the condition of zero space charge and unit electric potential at the subject electrode with all other electrodes at zero potential. The actual electric field, E, comes into play only in its effect on v. Charge trapping effects are neglected in this analysis.

Figure 7 shows the calculated induced charge signals due to the collection of electrons ($-q_0$) and holes ($+q_0$) created in localized interactions, such as single Compton scatter or photoelectric absorption, along the axis of the detector at various distances from the central electrode. In this calculation, the following empirical formula was used for v(E):

$$v(E) = \frac{\mu_o E}{1 + \frac{E}{E_o}}$$

where $\mu_0 = 4 \times 10^4$ cm^2/Vs, $E_0 = 270$ V/cm. This formula gives a good fit to experimental values measured at a temperature of 80 K. Sharp rises in the induced charge occur as the carriers make their final approach to the small central electrode. They effectively mark the arrival times of the charge packets. This provides an excellent way to determine the spatial distribution of charges deposited in the detector. This information can be used, for example, to discriminate gamma-ray events, which generally involve multiple Compton scattering processes, from charged particle events.

The induced charge signals from the shaped-field detector were observed using a storage oscilloscope connected to the output of a charge-sensitive preamplifier. Figure 8 shows some of the representative pulses obtained while the detector was irradiated with a ^{60}Co source. The detector was operated at a temperature of ≈ 77 K and a bias of 3200 V. Figure 8a shows an apparent single-site interaction while Fig. 8b and 8c clearly show multiple-site interactions. The pulse shapes agree well with the calculated ones (Fig. 7). Electronic discrimination of single- and multiple-site events can be performed in a relatively simple manner compared to that using coaxial detectors [8]. The low detector capacitance also enhances the signal-to-noise ratio in the wide-band system required for good pulse-shape measurements. The drift distances corresponding to the individual interactions in a complete event can be roughly estimated from the time of occurrence of the "steps" in the signals with respect to the signal start times.

Although the ability to discriminate single and multiple site interactions is a powerful feature, the usefulness of the shaped-field detector is compromised if the energy resolution is seriously degraded due to carrier trapping. As mentioned above, electron trapping effects are greatly enhanced for this detector geometry. This resulted in poor energy resolution as shown in the spectrum of ^{60}Co obtained at a detector temperature of ≈ 77 K (Fig 9). However, the resolution improved when the detector temperature was increased. At 125 K, a resolution of 4.9 keV FWHM was obtained for the 1.33 MeV peak. Similar temperature dependencies of energy resolutions have also been observed in reverse electrode coaxial detectors which showed significant trapping effects. The reduced trapping effect at higher temperatures is attributed to the more rapid release of trapped carriers. The spectra shown in Fig.9 were obtained using a Gaussian shaper with a peaking time of 16 μs. Because the carrier mobility at 125 K is less than half that at 77 K, the maximum signal rise time approached 2 μs and the ballistic deficit effect significantly degrades the energy resolution. Using a peaking time of 32 μs, a much improved resolution of 3.5 keV FWHM was obtained at a detector temperature of 125 K (Fig. 10) even though the electronic noise has risen to 1.7 keV FWHM due to noise contribution from the detector leakage

current which has increased to 150 pA. Although the energy resolution obtained is still considerably worse than that of coaxial detectors (≈ 2 keV), it is sufficiently good for many applications. One important test that remains to be done is to transform the present detector into a normal coaxial detector. The resultant energy resolution obtained will serve to 'calibrate' the material against those used for coaxial detectors in terms of electron traps, and will indicate whether or not significantly better materials are readily available for this application.

Conclusion

We have successfully fabricated a large volume germanium detector with a small collecting electrode. By selecting material with the appropriate impurity concentration and gradient, a proper drift field was established inside the detector for the collection of carriers. A full depletion capacitance of ≈ 1 pf was obtained. Very low noise operation is therefore possible, making such detectors good candidates for use in dark matter particle searches. For higher energy radiation, the nature of the pulse shapes obtained suggested that efficient pulse shape discrimination scheme can be implemented to distinguish between different types of radiation. We have shown that charge carrier trapping effects can be reduced by increasing the detector temperature. Further improvements may be obtained by selecting materials with higher impurity concentrations and gradients to generate higher drift fields, and by using material with lower electron trap concentrations. It may also be possible to use electronic corrections, including ballistic deficit correction [9], to improve the energy resolution.

Acknowledgments

We wish to thank B. Sadoulet for supplying us with information used in Fig. 2.

This work was supported by the Director's Office of Energy Research, Office of Health and Environmental Research, U.S. Department of Energy under Contract No. DE-AC03-76SF00098.

References

[1] G. R. Blumenthal, S. M. Faber, J. R. Primack and M. J. Rees, "Formation of Galaxies and Large-Scale Structure with Cold Dark Matter," *Nature* **311**, p. 517 (1984).

[2] B. Sadoulet, J. Rich, M. Spiro and D. O. Caldwell, "Testing the Weakly Interacting, Massive Particle Explanation of the Solar Neutrino Puzzle with Conventional Silicon Detectors," *Ap. J.* **324**, L75-L79 (1988).

[3] D. O. Caldwell, et al., "New Double Beta Decay Results and Constraints on Dark Matter," UCSB-ATP-87-3, to be published in *Phys. Rev. Lett.*

[4] P. N. Luke, N. W. Madden and F. S. Goulding, "Germanium Detectors with a Built-in Tranverse Drift Field," *IEEE Trans. Nucl. Sci.* **NS-32**, No. 1, p.457 (1985).

[5] P. N. Luke, "Low Noise Germanium Radial Drift Detector," *Nucl. Instr. Meth.* **A271**, p.567 (1988).

[6] E. E. Haller, W. L. Hansen and F. S. Goulding, "Physics of Ultra-pure Germanium," *Advances in Physics*, **Vol. 30**, No. 1, p.93 (1983).

[7] P. A. Tove and K. Falk, "Pulse Formation and Transit Time of Charge Carriers in Semiconductor Junction Detectors," *Nucl. Instr. Meth.* **29**, p.66 (1964).

[8] J. Roth, J. H. Primbsch and R. P. Lin, "Segmentation and Pulse Shape Discrimination Techniques for Rejecting Background in Germanium Detectors," *IEEE Trans. Nucl. Sci.* **NS-31**, No. 1, p.367 (1984).

[9] F. S. Goulding and D. A. Landis, "Ballistic Deficit Correction in Semiconductor Detector Spectrometers," *IEEE Trans. Nucl. Sci.* **NS-35**, No. 1, p.119 (1988).

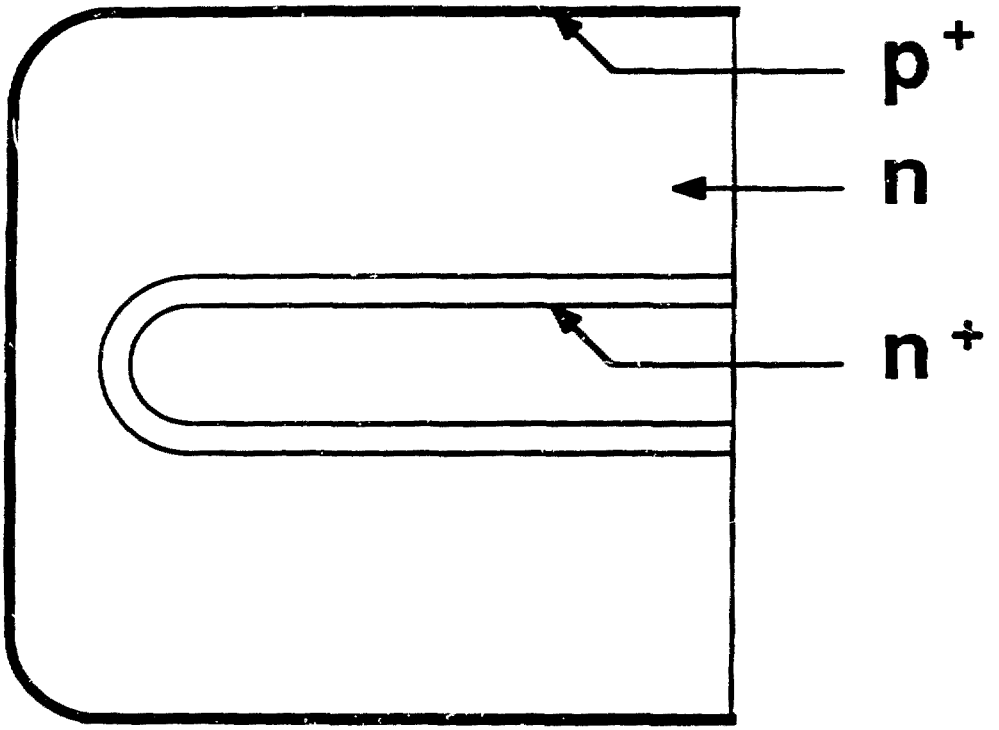

XBL 8810-3570

Fig. 1. Structure of a closed-end reverse electrode germanium coaxial detector.

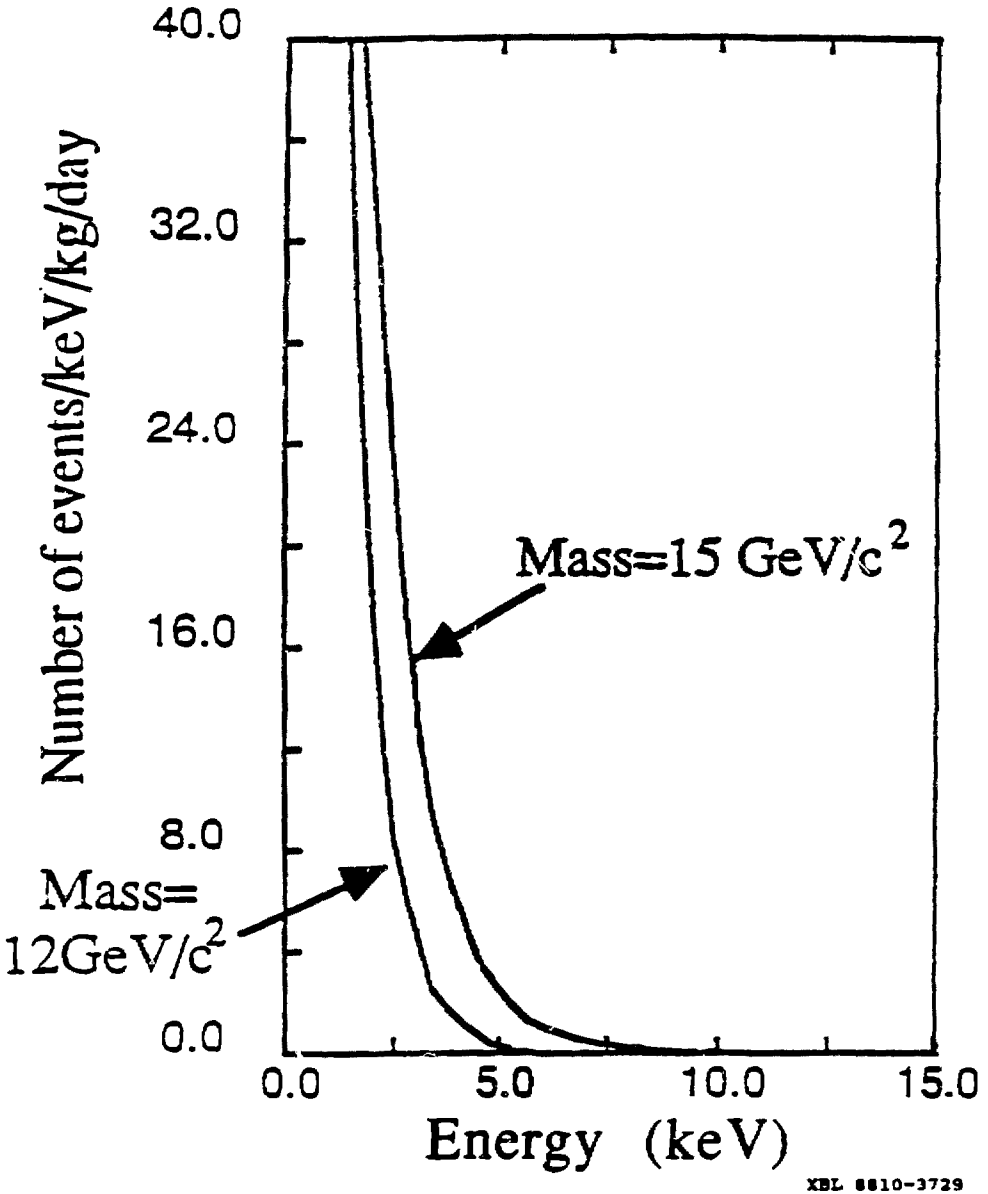

Fig. 2. Curves showing expected interaction rate and equivalent electron energy exchange in germanium for dark matter particles having 12 and 15 GeV/c^2 mass.

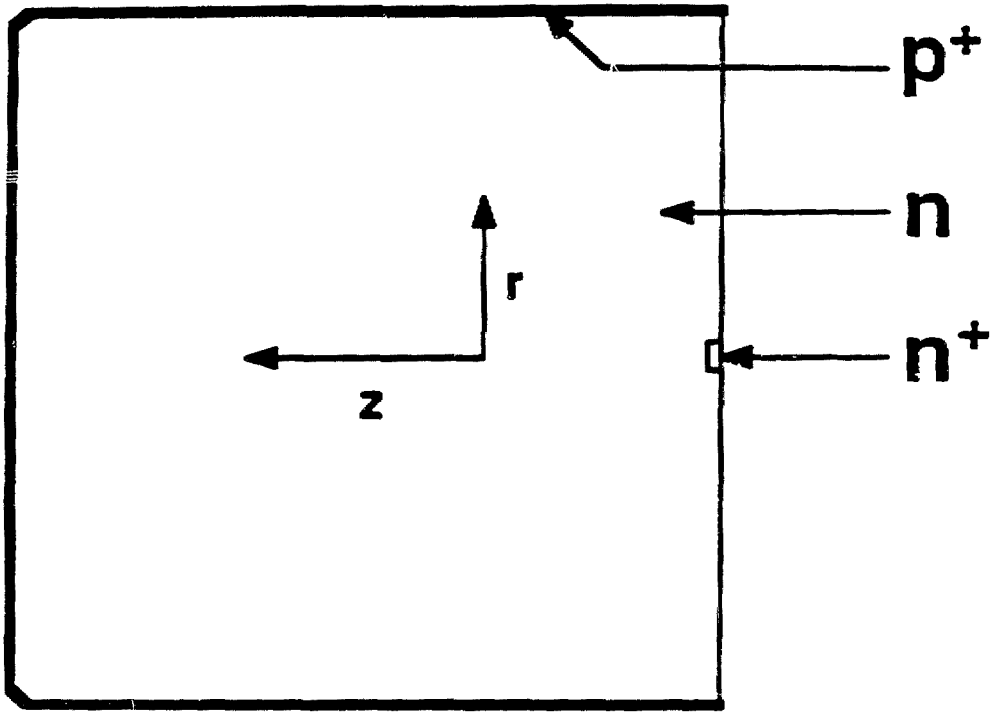

XBL 8810-3568

Fig. 3. Structure of the shaped-field detector.

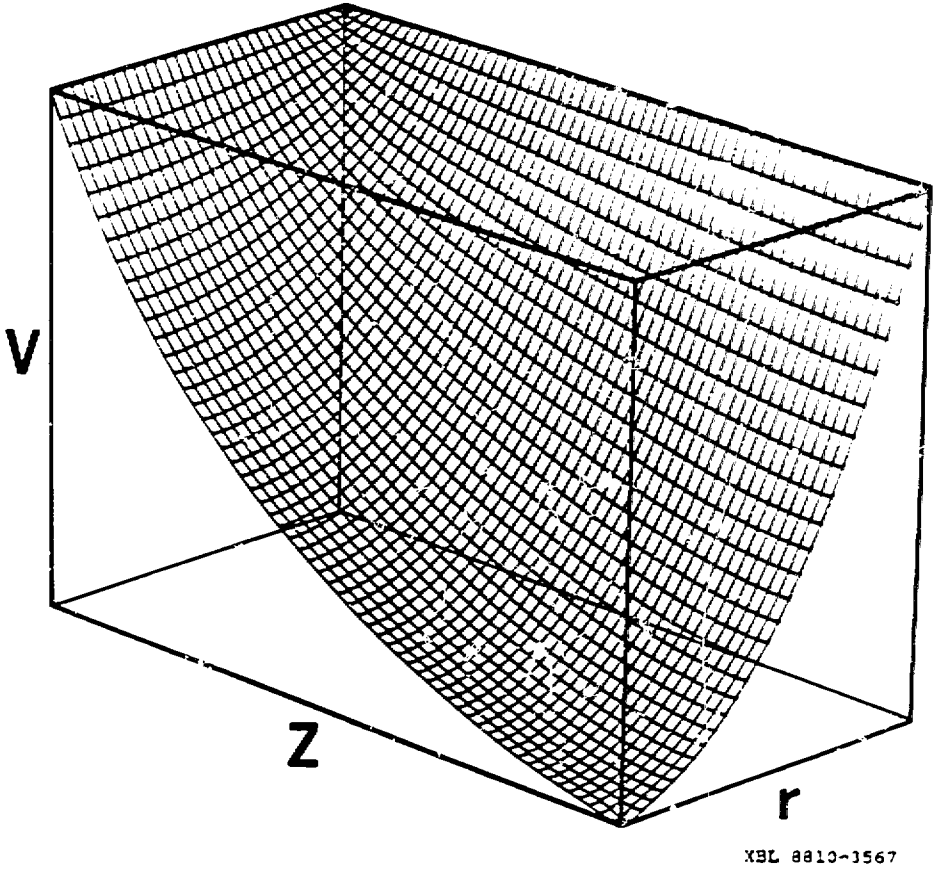

Fig. 4. Calculated potential distribution of the experimental shaped-field detector.

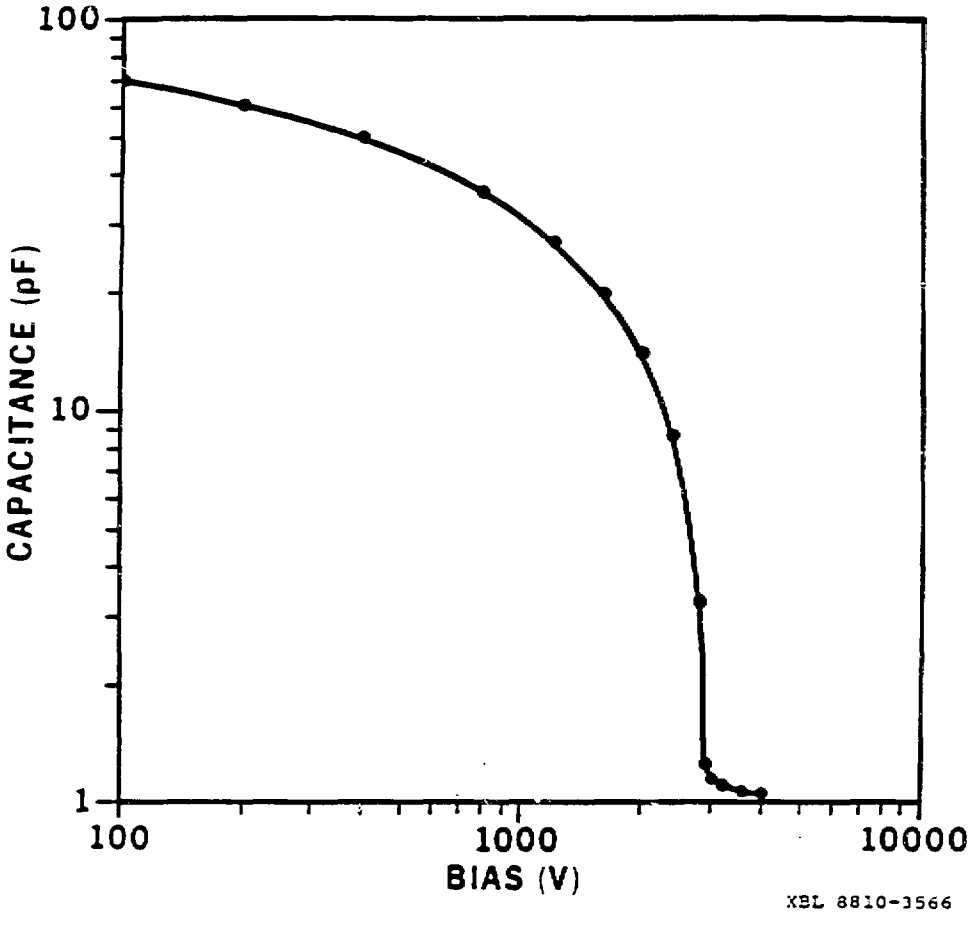

Fig. 5. Capacitance *vs.* bias voltage of the shaped-field detector.

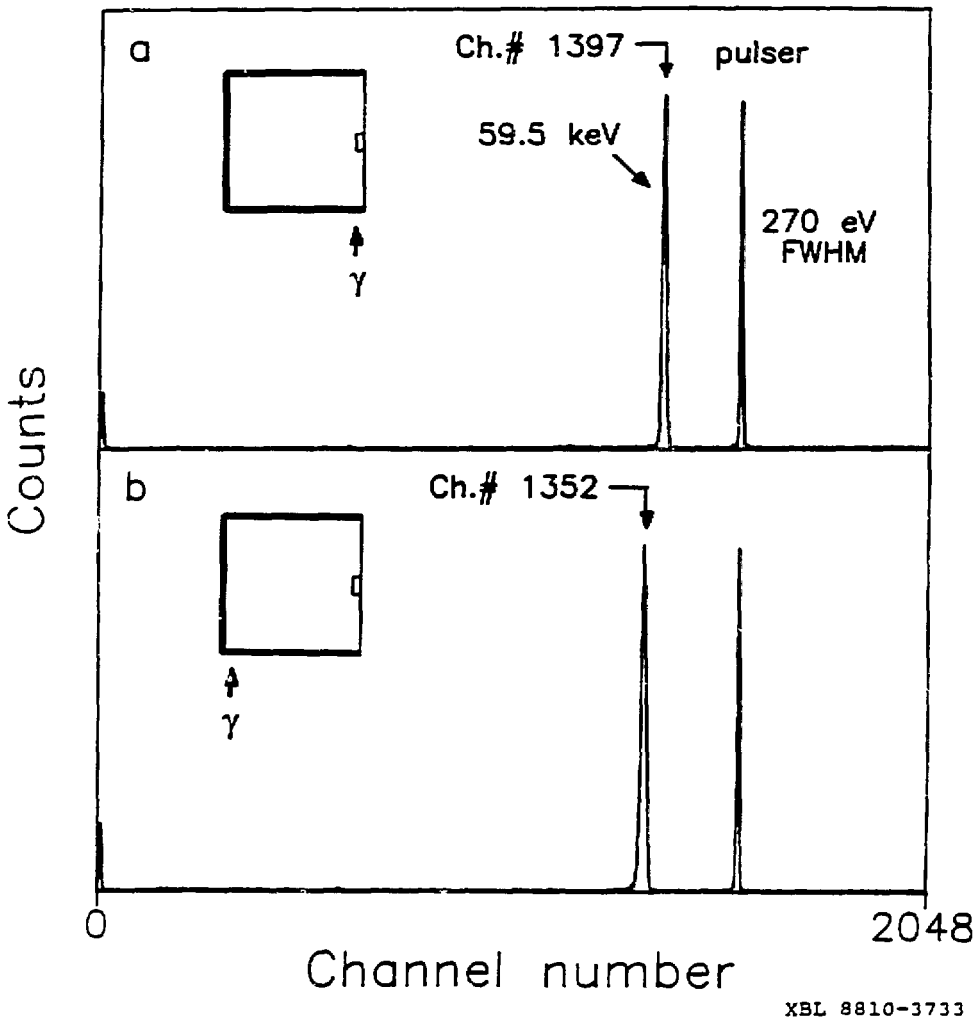

Fig. 6. Spectra obtained using a colliminated ^{241}Am 59.5 keV gamma ray source illuminating near the open end (a) and near the closed end (b) of the detector. The spectra were obtained with a detector bias of 3200 V, an amplifier peaking time of 8 μs, and no pulse height offsets.

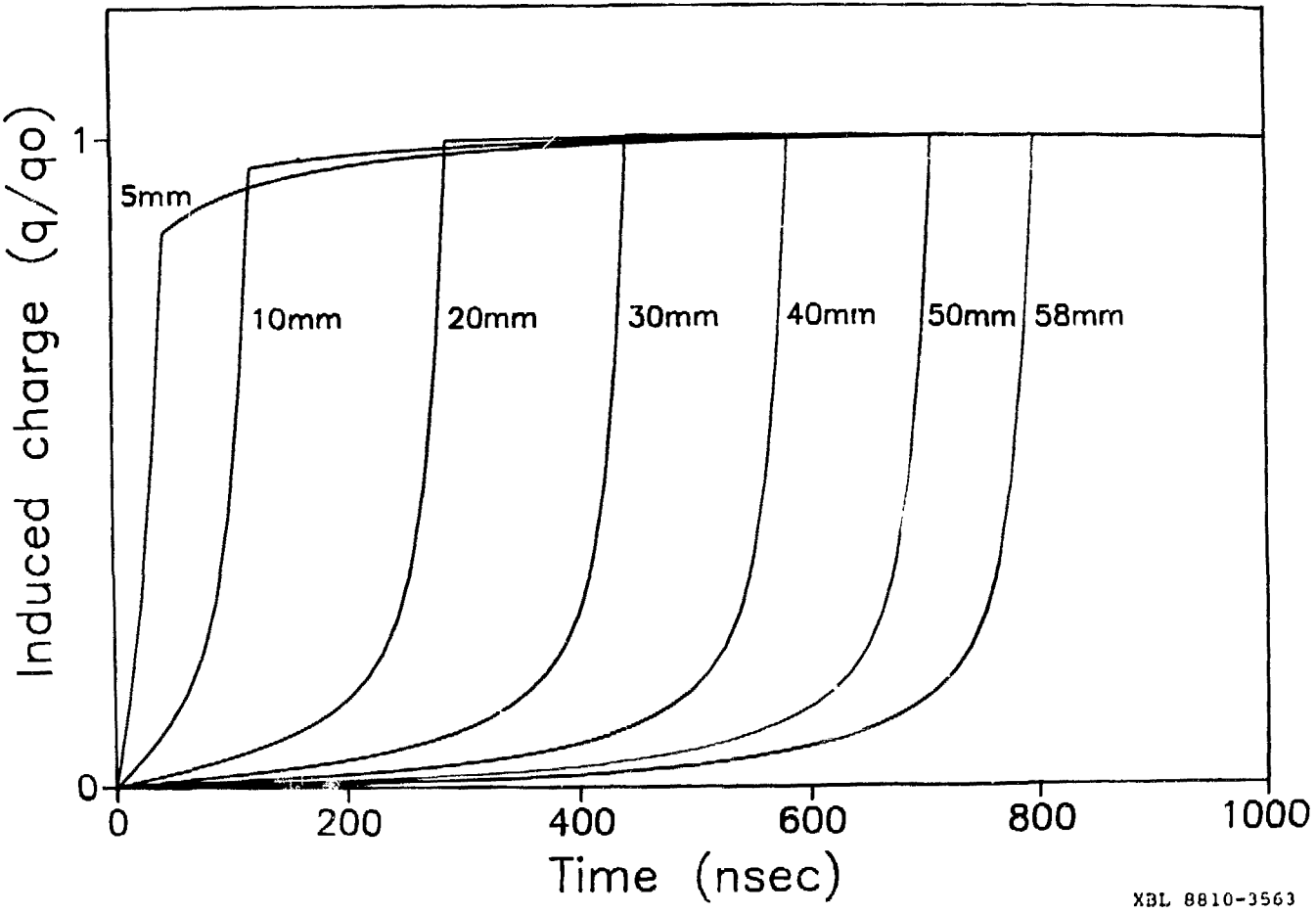

Fig. 7. Calculated pulse shapes due to point interactions along the detector axis at various distances fron the n^+ electrode.

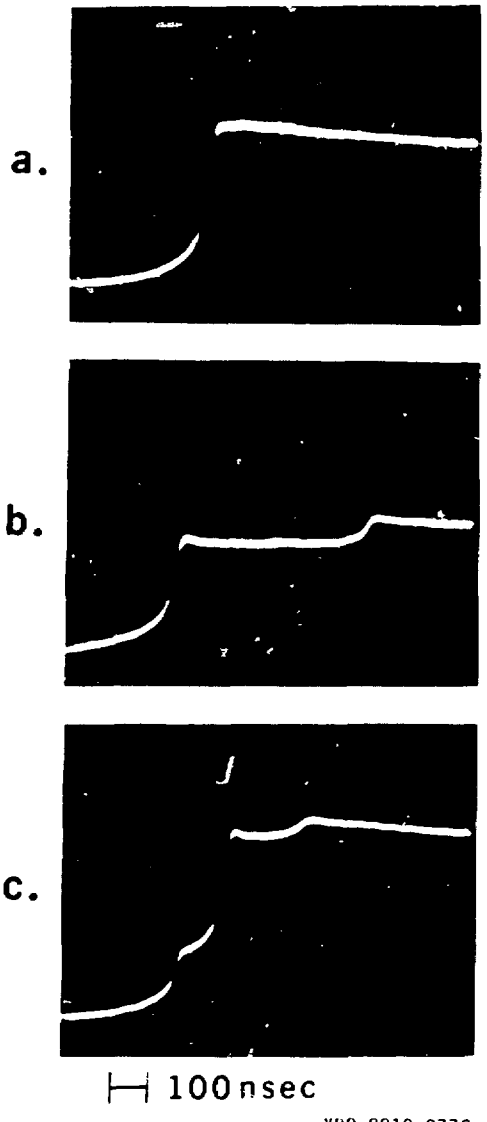

Fig. 8. Actual wide-band charge signals obtained from the detector irradiated with a ^{60}Co gamma ray source. Detector bias was 3200 V.

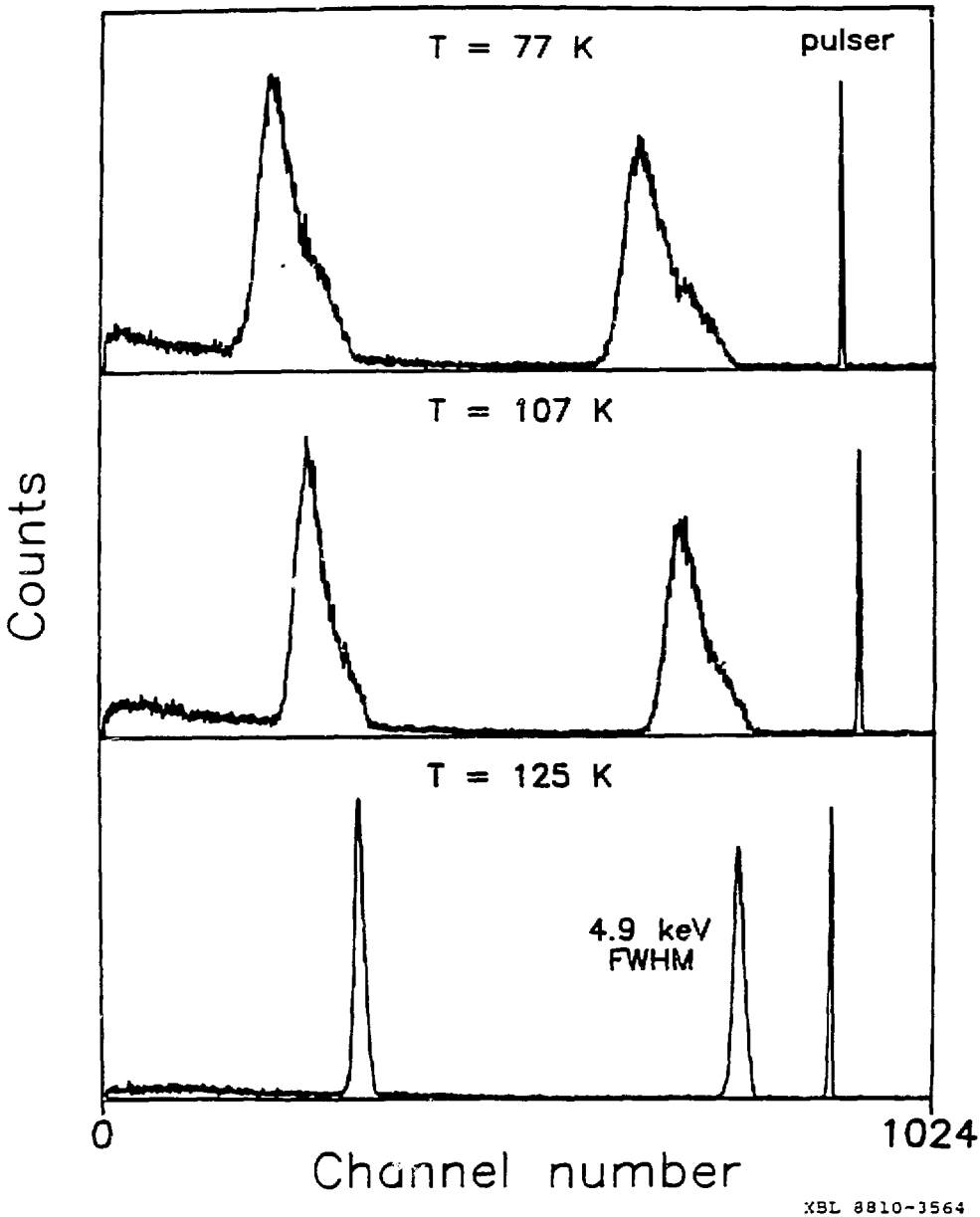

Fig. 9. ^{60}Co spectra obtained at different detector temperatures using an amplifier peaking time of 16 μs. Detector bias was 3200 V.

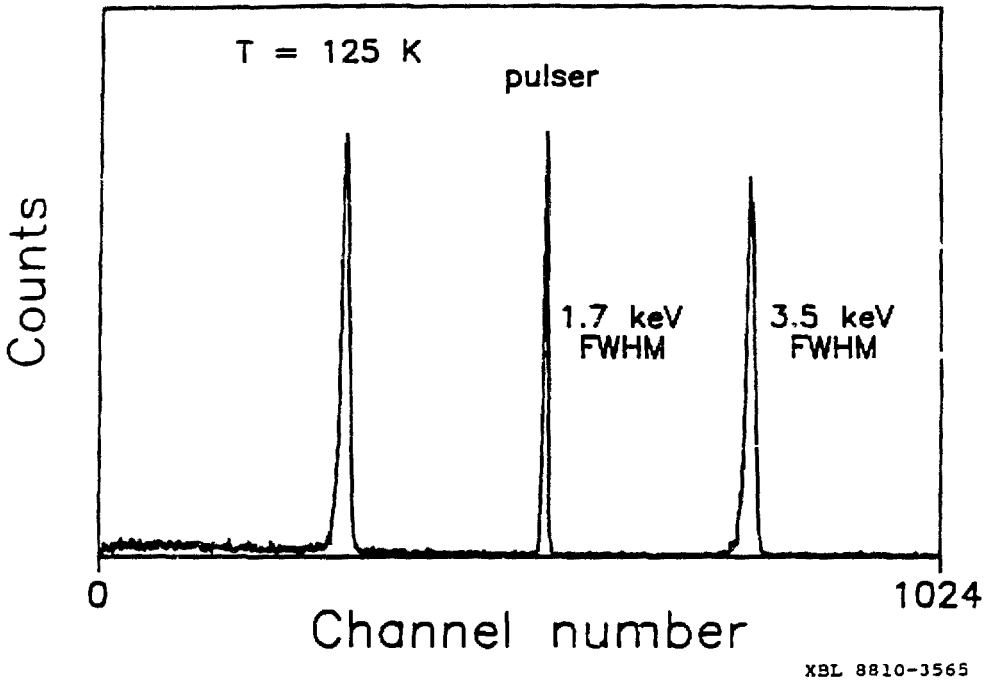

Fig. 10. ^{60}Co spectrum obtained at a detector temperature of 125 K using an amplifier peaking time of 32 μs and a detector bias of 3200 V.